Bull. Spec. Astrophys. Obs., 2002, 53, 78–94

The computation of the beam pattern of RATAN-600 with allowance for diffraction effects

E.K. Majorova

Special Astrophysical Observatory of the Russian AS, Nizhnij Arkhyz 369167, Russia

Received September 20, 2001; accepted October 19, 2001.

Abstract. Results are presented of calculation of the Mueller matrix elements of the radio telescope RATAN-600 that connect the Stokes parameters at the input and output of the antenna setup with allowing for the diffraction effects in the space between the primary and secondary mirrors. The proportion of spurious linear and circular polarization from the antenna is estimated when modeling passage of extended objects across the BP throughout the working wavelength range of RATAN-600 for the antenna being focused and with aberrations.

Key words: telescopes: radio — instrumentation: miscellaneous

1. Introduction

One of the most important performance characteristics of the radio telescope is the beam pattern (BP) of its antenna system. The antenna, which is an input device of any radio telescope, essentially affects the results of measuring cosmic radiation. A good knowledge of the antenna BP is required in studying extended objects, radio imaging of space objects by the method of aperture synthesis. Without knowing the cross-polarization components of the BP it is impossible to make qualitative polarization measurements.

The multiple enhancement of the RATAN-600 sensitivity called for a more detailed investigation into the BP far from its axis. More stringent requirements are placed upon the computation of the BP in intensity and polarization in connection with the scheduled studies of anisotropy of the microwave background at RATAN-600 on subdegree scales, the so-called Sakharov oscillations of the relic background (Parijskij, 2000).

The aim of the work was to analyse the already available experience of calculation of the RATAN-600 beam pattern, to create a programme on the basis of the existing programmes in which such effects as diffraction of electromagnetic waves in the space between the primary and secondary mirrors of the telescope, non-symmetry of the horn BPs (primary feeds) in the E and H planes would be taken into account. Besides, the problem was stated of estimation of the proportion of spurious polarization in observations of extended sources by means of calculation. Since the criterion of correctness of calculations is comparison with the experimental results, it was supposed to perform reference measurements of the BP in the main mode of the radio telescope performance, when only a part of the reflecting panels of the primary mirror is used, i.e. one of its sectors is in operation.

2. The history of the point

The RATAN-600 antenna is a variable profile antenna (VPA) in which the shape and width of the BP change depending on the observed source elevation. The beam pattern is moved in space not by rotation of the reflector on the whole, as in the case of paraboloids, but by changing the shape of the circular reflector (primary mirror) and by moving the secondary mirror on the radial railways. The electric vector of an incident wave when reflected from the primary and secondary mirrors rotates depending on the coordinates of the points of reflection, which leads to the appearance of cross-polarization components of the electric field and, in consequence, to the appearance of spurious polarization effects in the antenna (Esepkina et al., 1961).

A great number of papers are devoted to the investigation of the RATAN-600 BP. The investigations were carried out by way of calculations (Esepkina et al., 1979a,b; 1980; 1982), by way of optical modeling (Esepkina et al., 1977, Korzhavin, 1977) and also with the aid of observations of intense cosmic sources (Temirova, 1983; 1985; Abramov & Vinyajkin, 1985), which made it possible to have a sufficiently complete idea of the BP in both intensity and polarization.

The papers by Esepkina et al. (1961, 1972), in which the principal formulae were derived and the two-dimensional BP of a radio telescope of type of RATAN-600 was computed for the first time, should

be referred to the basic papers that formed the foundation of all subsequent theoretical studies of the VPA BP. The BPs of such antennae were shown to have both main and spurious polarizations. To investigate the latter, Esepkina (1972) suggests the use of the Mueller technique. The elements of the Mueller matrix connect the Stokes parameters at the input and output of antenna setup. The expressions for them derived in the above-mentioned paper were used further to compute the polarization characteristics of the Big Pulkovo Radio Telescope (Bakhvalov et al., 1973) and of the radio telescope RATAN-600 (Esepkina et al., 1979b; 1982).

In the papers by Esepkina et al. (1979b; 1980; 1982) the BPs and the Mueller matrix elements of the radio telescope RATAN-600 were calculated with antenna aberrations and without them. The BPs were computed by the aperture method (Esepkina et al., 1961). The components of the fields in the apertures of the secondary and main mirrors were found in an approximation of geometric optics with the use of the matrix method which is convenient in computing multimirror antennae. A "scalar" horn with symmetric beam patterns in the E and H planes was considered as the primary feed of a non-symmetric parabolic cylinder. In the calculations they were assumed to be decreasing in a cosine manner. The beam patterns were computed at the computer centre of MSU. The greater part of them are stored at St. Petersburg Branch of SAO in the form of graphs.

A similar method of computation of the BP was employed in the programmes of A.N. Korzhavin who had preliminarily investigated in detail the polarization characteristics of the secondary mirror, derived formulae for the electric vector projections in a cylindrical wave formed by the non-symmetric parabolic cylinder, analysed the contribution of the secondary and primary mirrors to the polarization effects in observations at different elevations (Korzhavin, 1979). Based on the derived formulae, a programme (GSOBX1) was written which enables the field distribution in the aperture of the secondary mirror to be computed with allowance made for its geometric and structural characteristics, proceeding from the BPs of the primary feeds. As a subprogramme it is incorporated in the main programme of computing the two-dimensional BP which is used to calculate the Mueller matrix elements M_{11} and M_{41} and also the BP of the right and left polarizations M_R, M_L. The programme enables calculation of the RATAN-600 BP under the condition of operation of one sector or the "South sector with the flat reflector". However, the programme does not take account of the vertical size of the reflecting panels of the primary mirror, the antenna aperture is represented by infinitely thin ring, which causes loss of information about the envelope of the vertical BP of the radio telescope.

A different algorithm was suggested in the paper by Gelfreikh (1977). Its essence is the fact that the primary mirror was considered as a multielement interferometer whose elements are the panels that compose the reflecting surface. The formulae for the calculation of positions of the panels with respect to the focus were derived in the paper by Gelfreikh (1972). The programme used to implement the given algorithm calculates the two-dimensional BP in intensity and circular polarization with arbitrary displacement of the feed from the focus. However, the programme does not take into account the secondary mirror and its polarization effects. The character of the field distribution over the aperture is specified analytically. The vertical size of the panel is allowed for in the paper by Gelfreikh, Opeikina (2000). The programme is convenient for computing the BP of the radio telescope in the modes "Relay" (Golubchina, Golubchin, 1981) and radio heliograph (Bogod et al., 1988) and also for assessment of the effects the antenna setting errors have on the shape and quality of the BP.

Review of the given papers shows that we presently have a sufficiently complete idea of the RATAN-600 BP. Besides, there exist working programmes by G.B. Gelfreikh and A.N. Korzhavin with the aid of which one can compute individual Mueller matrices for different antenna configurations. The programme of Korzhavin was subsequently rewritten from FORTRAN to C and included in the FADPS package (Verkhodanov et al., 1993).

When computing the RATAN-600 BP, the diffraction effects in the space between the secondary and primary mirrors, the influence of the non-symmetry of the BP of the horns in the E and H planes on the polarization characteristics of the radio telescope and the effects the reflection of electromagnetic waves from the Earth's surface have on the BP structure at long wavelengths were left out of account. In the present paper we dwell upon the first two points.

3. The computation of the RATAN-600 BP with allowance for diffraction effects

The antenna of the radio telescope changes the state of polarization of the cosmic radiation being received. The relation between the Stokes parameters at the input and output of the antenna setup can be represented (Esepkina, 1972) as

$$\begin{bmatrix} I \\ Q \\ U \\ V \end{bmatrix} = \begin{bmatrix} M_{11} & M_{12} & M_{13} & M_{14} \\ M_{21} & M_{22} & M_{23} & M_{24} \\ M_{31} & M_{32} & M_{33} & M_{34} \\ M_{41} & M_{42} & M_{43} & M_{44} \end{bmatrix} \begin{bmatrix} I_0 \\ Q_0 \\ U_0 \\ V_0 \end{bmatrix},$$

where I_0, Q_0, U_0, V_0 are the Stokes parameters of the input radiation. I, Q, U, V are the Stokes pa-

rameters of the output radiation, M is the Mueller matrix which defines polarization characteristics of the antenna for a point source. Parameters I, I_0 determine the intensity of radiation, parameters Q, U, V, Q_0, U_0, V_0 are the polarization components of radiation.

Element M_{11} characterizes the power BP for an unpolarized source of radio emission, M_{22} for a linearly polarized source with 100% polarization, elements M_{41}, M_{14} determine the diagrams of spurious circular polarization for an unpolarized source of radio emission, elements $M_{21}, M_{12}, M_{13}, M_{31}$ for spurious linear polarization, elements M_{23}, M_{32} characterize variations of the position angle of linearly polarized radiation. It was shown by Esepkina et al. (1979b) that with the beam patterns of the primary feeds, when the E and H panels are symmetric, only the diagonal elements $(M_{11}, M_{22}, M_{33}, M_{44})$ and the elements that characterize transition to each other of parameters I and V (M_{14}, M_{41}) and Q and U (M_{23}, M_{32}) are different from zero, the values of M_{11} being coincident with M_{44}, and M_{22} with M_{33}.

We will now dwell upon the computation of matrix element M_{11}, which is the power BP of the radio telescope for unpolarized radiation. We use the formula of Esepkina et al. (1972) for the computation

$$M_{11} = [(f_{xx}f^*_{xx} + f_{yx}f^*_{yx}) + (f_{xy}f^*_{xy} + f_{yy}f^*_{yy})]/2, \quad (1)$$

where f_{xx} and f_{xy} are the beam patterns for the main polarization and cross-polarization, when the field of the feed is vertically polarized, f_{yy} and f_{yx} are the beam patterns for the main polarization and cross-polarization, when the field of the feed is horizontally polarized.

Let us consider the main mode of operation of RATAN-600 with one of the sectors of the circular antenna. The geometry of the antenna is such that if beam path in the horizontal plane is fitted by an approximation of geometric optics, then the approximation of geometric optics is not satisfied for part of the working wavelength range in the vertical section of the antenna in the space between the secondary and primary mirrors. Calculation of the field distribution in the vertical aperture of the primary mirror has to be performed in a diffraction approximation, as it was done when investigating the RATAN-600 periscopic system (Majorova, Stotsky, 1981) and when computing the effective area of the radio telescope (Majorova, Stotsky, 1982). The diffraction effects in the Fresnel zone were also taken into account when choosing the optimum sizes of the telescope mirrors (Braude et al., 1972) and in the calculation of the BPs of the panels of the primary mirror in the vertical plane. To compute the latter, A.N. Korzhavin wrote a separate programme in which the above-mentioned programme, GSOBX1, was included as a subprogramme. Provision for the diffraction effects in the Fresnel zone shows that with the same in-phase field distribution in the vertical aperture of the secondary mirror the amplitude-phase field distribution in the vertical aperture of the primary mirror is strongly dependent on the wavelength and the elevation of a source observed (Majorova, Stotsky, 1981).

To compute the orthogonal components of the electric field A_{ij}, we use the formula

$$A_{ij}(\varepsilon, u) = \frac{1}{\sqrt{\lambda\rho(\varepsilon)}} \int_{-b/2}^{b/2} E_{ij}(\varepsilon, t) e^{\frac{-j\pi(u-t)^2}{\lambda\rho}} dt, \quad (2)$$

where E_{ij} are the components of the main polarization (E_{xx}, E_{yy}) and cross-polarization (E_{xy}, E_{yx}) of the electric vector in the vertical aperture of the secondary mirror, b is the vertical size of the secondary mirror, ρ is the distance of the primary mirror aperture in the horizontal plane from the focus, u and ε are the polar coordinates in the aperture plane of the main mirror, λ is the wavelength.

The electric vector components in the secondary mirror aperture with the vertical (E_{xx}, E_{xy}) and horizontal (E_{yy}, E_{yx}) polarizations of the feed field we computed by the programme GSOBX1. The beam patterns of the primary feeds in the E and H planes were assumed to be symmetrical. In observations with the "scalar" horns this condition is satisfied quite well (Parijskij et al., 1973). The programme GSOBX1 was modified to calculate both polarizations on the basis of the formulae presented in the paper by Korzhavin (1979).

Taking into account that the components of the main (A_{xx}, A_{yy}) and cross-polarization (A_{xy}, A_{yx}) components of the electric field in the vertical aperture of the primary mirror are complex values

$$A_{ij}(\varepsilon, u) = F_{ij}(\varepsilon, u) e^{j\phi_{ij}(\varepsilon,u)} = F^r_{ij}(\varepsilon, u) + jF^i_{ij}(\varepsilon, u), \quad (3)$$

the formulae for calculation of the BP of the main polarization and cross-polarization presented in the paper by Esepkina et al. (1979b) can be rewritten in the following form

$$f_{xx}(\theta, \psi) = \frac{1}{f_{xx}(0,0)} \int_{-\varepsilon_0}^{\varepsilon_0} \int_{-u_0}^{u_0} (F_{xx}(\varepsilon, u) e^{\phi_{xx}(\varepsilon,u)} \cos\varepsilon - F_{xy}(\varepsilon, u) e^{j\phi_{xy}(\varepsilon,u)} \sin\varepsilon) e^{j\Phi(\varepsilon,u,\theta,\psi)} du d\varepsilon, \quad (4)$$

$$f_{xy}(\theta, \psi) = \frac{1}{f_{xx}(0,0)} \int_{-\varepsilon_0}^{\varepsilon_0} \int_{-u_0}^{u_0} (F_{xx}(\varepsilon, u) e^{\phi_{xx}(\varepsilon,u)} \sin\varepsilon + F_{xy}(\varepsilon, u) e^{j\phi_{xy}(\varepsilon,u)} \cos\varepsilon) e^{j\Phi(\varepsilon,u,\theta,\psi)} du d\varepsilon, \quad (5)$$

$$f_{yy}(\theta, \psi) =$$

$$\frac{1}{f_{yy}(0,0)}\int_{-\varepsilon_0}^{\varepsilon_0}\int_{-u_0}^{u_0}(F_{yy}(\varepsilon,u)e^{\phi_{yy}(\varepsilon,u)}\sin\varepsilon \quad + \quad F_{yx}(\varepsilon,u)e^{j\phi_{yx}(\varepsilon,u)}\cos\varepsilon)e^{j\Phi(\varepsilon,u,\theta,\psi)}dud\varepsilon, \tag{6}$$

$$f_{yx}(\theta,\psi) \quad =$$

$$\frac{1}{f_{yy}(0,0)}\int_{-\varepsilon_0}^{\varepsilon_0}\int_{-u_0}^{u_0}(F_{yy}(\varepsilon,u)e^{\phi_{yy}(\varepsilon,u)}\cos\varepsilon \quad - \quad F_{yx}(\varepsilon,u)e^{j\phi_{yx}(\varepsilon,u)}\sin\varepsilon)e^{j\Phi(\varepsilon,u,\theta,\psi)}dud\varepsilon, \tag{7}$$

Write expression for the phase Φ as:

$$\Phi(\varepsilon,u,\theta,\psi) \quad = \quad -\frac{2\pi}{\lambda}[\frac{P}{\sin h}(X\sin\varepsilon+Y\cos\varepsilon)+u(X\sin\varepsilon+Y)], \tag{8}$$

$X=\sin\theta\sin\psi, Y=\sin\theta\cos\psi$, where θ, ψ are the angular spherical coordinates of the point of observation, h is the height of the observed source, P is the antenna parameter. When one sector of the radio telescope is in operation, the antenna aperture is a part of the ring $2u_0$ in width and an angular size $2\varepsilon_0$. $2u_0=H\cos(h/2)$, where H is the height of the panel, $2\varepsilon_0$ is defined by the number of the panels set and by the character of irradiation of the primary mirror.

The phase Φ was computed via formula (8), which is somewhat different from the formula given by Esepkina et al (1979b):

$$\Phi(\varepsilon,u,\theta,\psi) = -\frac{2\pi}{\lambda}[(\frac{P}{\sin h}+u)(X\sin\varepsilon+Y\cos\varepsilon)]. \tag{9}$$

Here we propose a trade-off alternative of the approaches implemented in the paper by Esepkina et al. (1961; 1979b). Because the field distribution in the primary mirror aperture depends on the two coordinates (ε and u), we do not succeed in separation of the variables and representing the double integral in formulae (4—7) by the product of two integrals, as it was done in the paper by Esepkina et al. (1961). Taking into account, however, that the field distribution in the vertical sections of the antenna is only slightly dependent on the coordinate ε, we introduce some changes in the calculation of the phase Φ. Fig. 1 illustrates that, as a result of this approach, the computed BP is in a better agreement with experimental.

Fig. 1 shows maximum values of the beam pattern $M_{11}{}^{max}$ in different horizontal sections ($Y\neq 0$) normalized to the maximum BP in the central horizontal section (Y=0, $\psi=90°$) at the wavelength λ7.6 cm (a) and λ3.9 cm (b). The positions of these sections with respect to the central one in angular measure (θ) are laid off as abscissa. The primary feed at λ 7.6 cm was at the focus of the antenna ($\Delta x=0$), at λ 3.9 cm it was displaced from the focus by $\Delta x=7.8\lambda$. The phase Φ was computed via formula (8) — curve 1, and (9) — curve 2. The dashed line shows the relationships $M_{11}{}^{max}(\theta)$ calculated with no allowance for the vertical size of the panel, the triangles are the experimental values of $M_{11}{}^{max}$ obtained from observations of the point source PKS1830-211 ($h=25°$) as it passed across the RATAN-600 BP in different horizontal sections. Note that the relations $M_{11}{}^{max}(\theta)$ for the focused antenna are the vertical BPs of the radio telescope because the BP maxima of different horizontal sections lie in one vertical plane (X=0, ψ=0).

As one can see from the figure, the experimental points fit well curves 1 computed from formulae (1 — 8) for both the focused antenna (λ 7.6 cm) and the antenna with transverse aberrations (λ 3.9 cm). The BPs at λ7.6 cm computed from formula (9) (curve 2 in Fig. 1a) has discrepancies with the experimental point at the edges, while the relation $M_{11}{}^{max}(\theta)$ at λ3.9 cm (curve 2 in Fig. 1b) does not fit the experimental points throughout the range of variation of angle θ. Besides, the BPs computed via formula (9) (curves 2) and those calculated with no provision for the vertical size of the panel (dashed line) coincide, although the vertical size of the panel was taken into account when the former were computed.

Similar curves were computed for the height $h=86°$ (Fig. 2). Experimental points were obtained from observations of the point source TEX2005+403 ($h=86°$). As it turned out, all the curves at this height practically coincide and are fairly consistent with the values of $M_{11}{}^{max}$ derived in observations.

Fig. 3 displays the computed beam patterns $M_{11}(\theta)$ of the radio telescope for $h=10°,30°,60°,90°$. The BPs were computed in an approximation of geometrical optics as functions of $(\pi P\sin\theta/\lambda)$. In this approximation the field distribution over the vertical aperture of the panel is consistent to an accuracy of the factor $1/\rho$ with the field distribution over the vertical aperture of a non-symmetrical parabolic cylinder. It can be seen from the plots presented in Fig. 3 that the BPs computed by formula (9) with allowance made for the vertical size of the panel (curves 2) coincide with those computed with no provision for the vertical size of the panel (curves 3). Besides, they turn to be more extended than the BPs computed by formula (8) (curves 1). The differences manifest themselves the stronger the lower is the elevation of the source. This is connected with the fact that the value of $P/\sin h$ at low elevations is orders of magnitude higher than the values of u_0, and the count accuracy is insufficient for taking account of the influence of the vertical size of the panel.

A number of observers noted that the measured vertical BPs at low angles turn out to be less extended than it follows from the computations of Esepkina et al. (1979b). The discrepancy between theory and

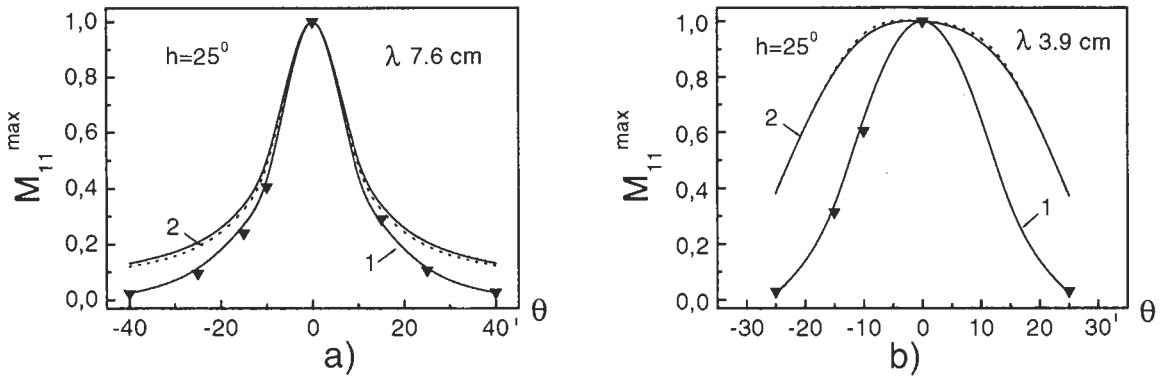

Figure 1: *Maximum values of the BP in different horizontal sections* $M_{11}{}^{max}$ *normalized to the maximum of the BP in the central horizontal section (Y=0,* $\psi = 90°$*) for the wavelength* $\lambda 7.6$ *cm* (Δx=0) — *(a) and for the wavelength* $\lambda 3.9$ *cm* ($\Delta x = 7.8\lambda$) — *(b). Curves 1 — phase* Φ *is computed by formula (8), curves 2 — by formula (9). The dotted lines — (BP) is computed with no provision for the vertical size of the panel, the triangles are the experimental values of* $M_{11}{}^{max}$ *derived from observations of the source PKS1830-211* ($h = 25°$).

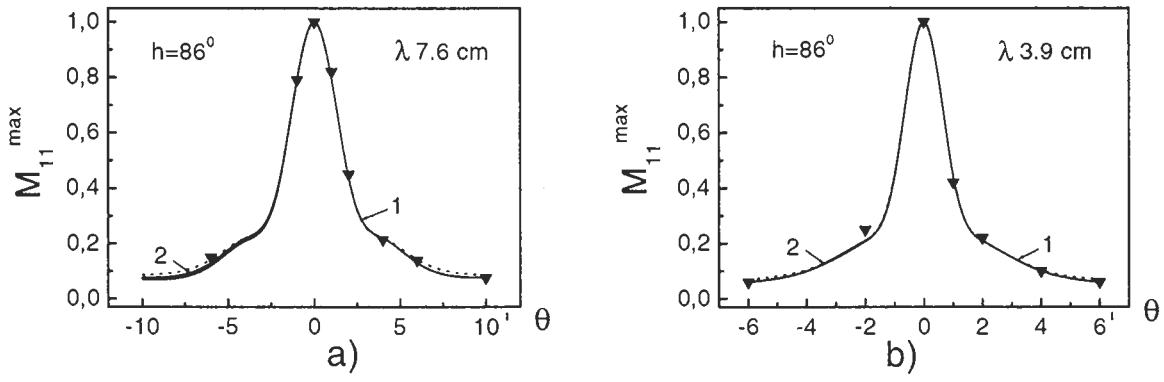

Figure 2: *The same as in Fig.1 for the source TEX2005+403 (* $h = 86°$*).*

experiment can be revealed from comparing the results obtained by Temirova (1983) and Esepkina et al. (1979b). The measured vertical BPs (Temirova, 1983) at low elevations ($h \leq 30°$) at a level of 0.2 and lower prove to be much lower than the BPs calculated by Esepkina et al. (1979b), while at a half-power level no discrepancies are observed.

Let us dwell on the influence the diffraction effects have upon the shape of the RATAN-600 BP. Fig. 4 shows the vertical BPs computed with allowance made for the diffraction effects in the space between the secondary and main mirrors at the wavelength λ = 4 cm, 8 cm, 16 cm and 32 cm (curves 1, 2, 3, 4, respectively). The BPs were computed by formulae (1 — 8) for the elevations $h = 10°, 30°, 60°, 90°$. The vertical size of the panel was assumed to be 11.1 m. The BPs of the primary feeds were specified to be equal for all wavelengths. Since the vertical BPs are presented as functions of ($\pi P \sin\theta/\lambda$), they must not depend on the wavelength, provided that the approximation of geometrical optics is satisfied. The curves in Fig. 4 are different, which is caused by the influence the diffraction effects have on the shape of the BP. This influence is the most pronounced at low elevations. The beam pattern not only narrows at the wavelength λ32 cm at $h = 10°$, but also its maximum is displaced. The influence of the diffraction effects is less pronounced at medium and high angles, but here too the BP shape is somewhat different at different wavelengths. In order to show these variations at the elevations $h = 30°, 60°, 90°$, the normalized power BPs are given below the levels 0.5, 0.3 and 0.2, respectively.

Figs. 5 and 6 present the isophotes of element M_{11} (of the power BP) at λ 32 cm for the source elevations $h = 10°, 30°, 60°$. In Fig. 5 are displayed the beam patterns for the focused antenna (left) and the BPs for the transverse displacement of the primary feed

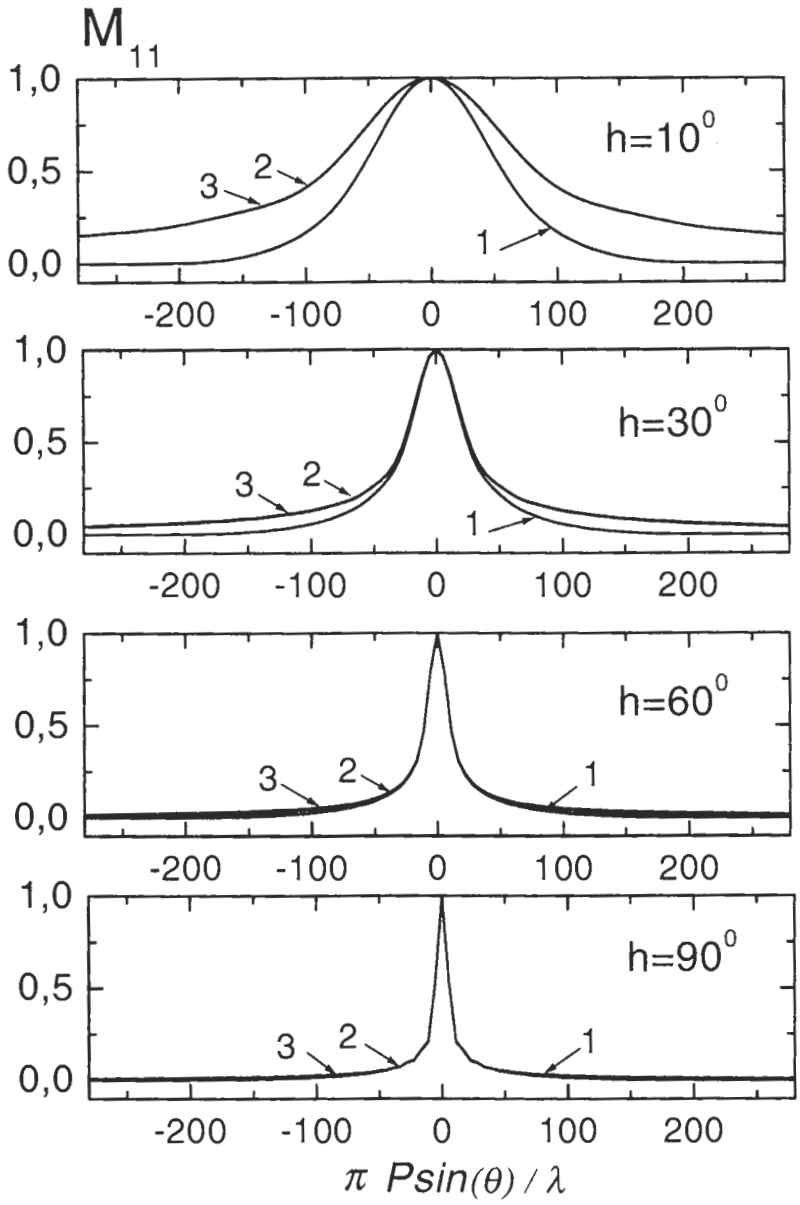

Figure 3: *Vertical BPs calculated in the approximation of geometrical optics. Curves 1 — the phase* Φ *is computed by formula (8), curves 2 — from formula (9), curves 3 — the calculation of the BP with no allowance for the vertical size of the panel.*

from the focus ($\Delta x = 5\lambda$). The BPs were computed in a diffraction approximation via formulae (1)— (8) (Fig. 5a, 6a), in an approximation of geometrical optics by means of formula (8) for the computation of phases (Fig. 5b, 6b) and in an approximation of geometrical optics by formula (9) (Fig. 5c, 6c), as it was done in the paper by Esepkina et al. (1979b). The BPs are normalized to $M_{11}(0,0)$, the isophotes are drawn with a step of 0.1.

It can be seen from the figures that at low elevations the size and shape of the beam patterns calculated in the diffraction approximation and in the approximation of geometrical optics with the use of formulae (8) and (9) are different. The differences are the greater the smaller is the elevation of the source. When passing from Figs. 5c, 6c to Figs. 5b, 6b and, at

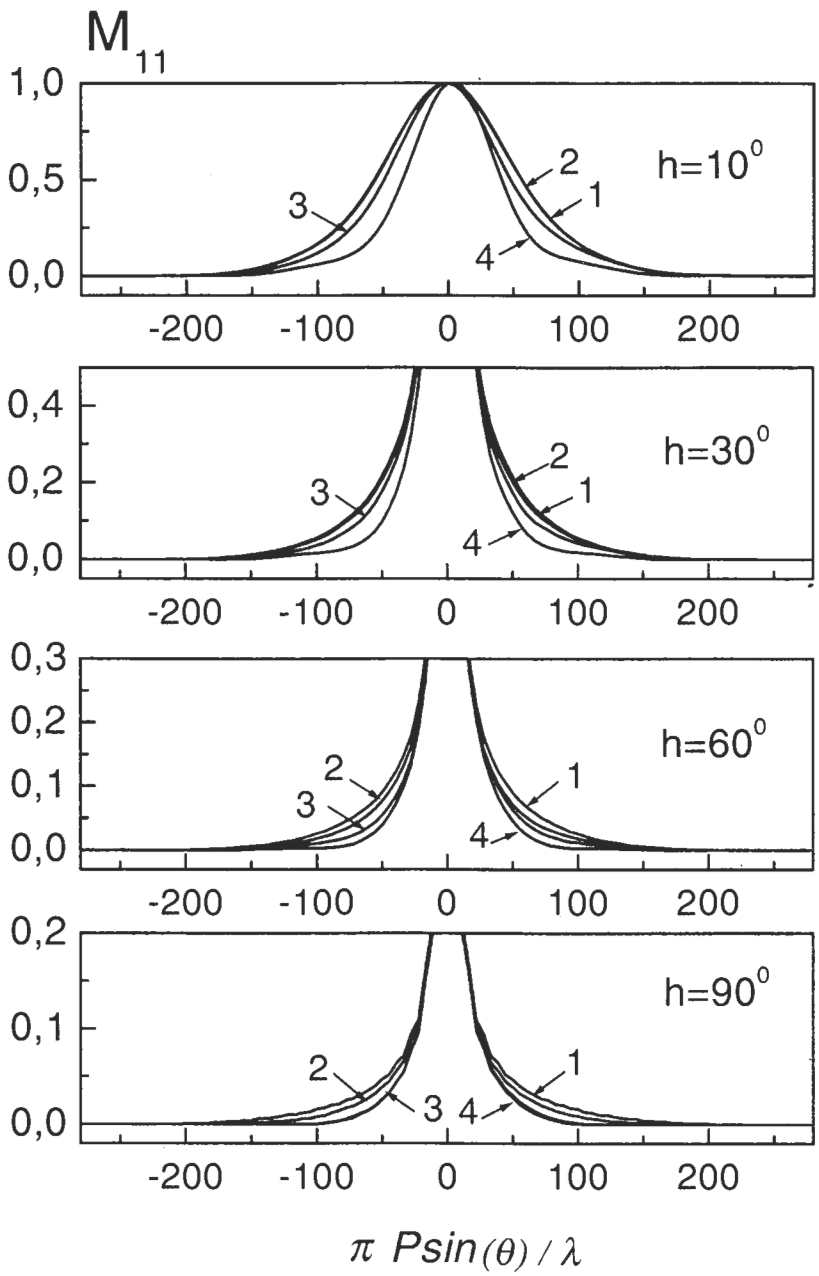

Figure 4: *Vertical BPs in the diffraction approximation at λ4 cm, 8 cm, 16 cm and 32 cm (curves 1, 2, 3, 4, respectively).*

last, to Figs. 5a, 6a, the solid angle taken by the BP decreases; the pattern becomes less extended. This effect is observed both with the focused antenna and in the presence of aberrations.

At elevations close to $h = 90°$ the beam patterns computed in the diffraction approximation and geometrical optics approximation practically coincide as well as do the results of calculations via formulae (8) and (9). This is connected with the fact that near the zenith the BP shape in the vertical plane is defined by the depth of the antenna aperture, which is a few times the size of the panel at these elevations; so the effect of the size of the panel becomes negligibly small. The influence of the panel envelope on the BP shape increases with the decrease of the source

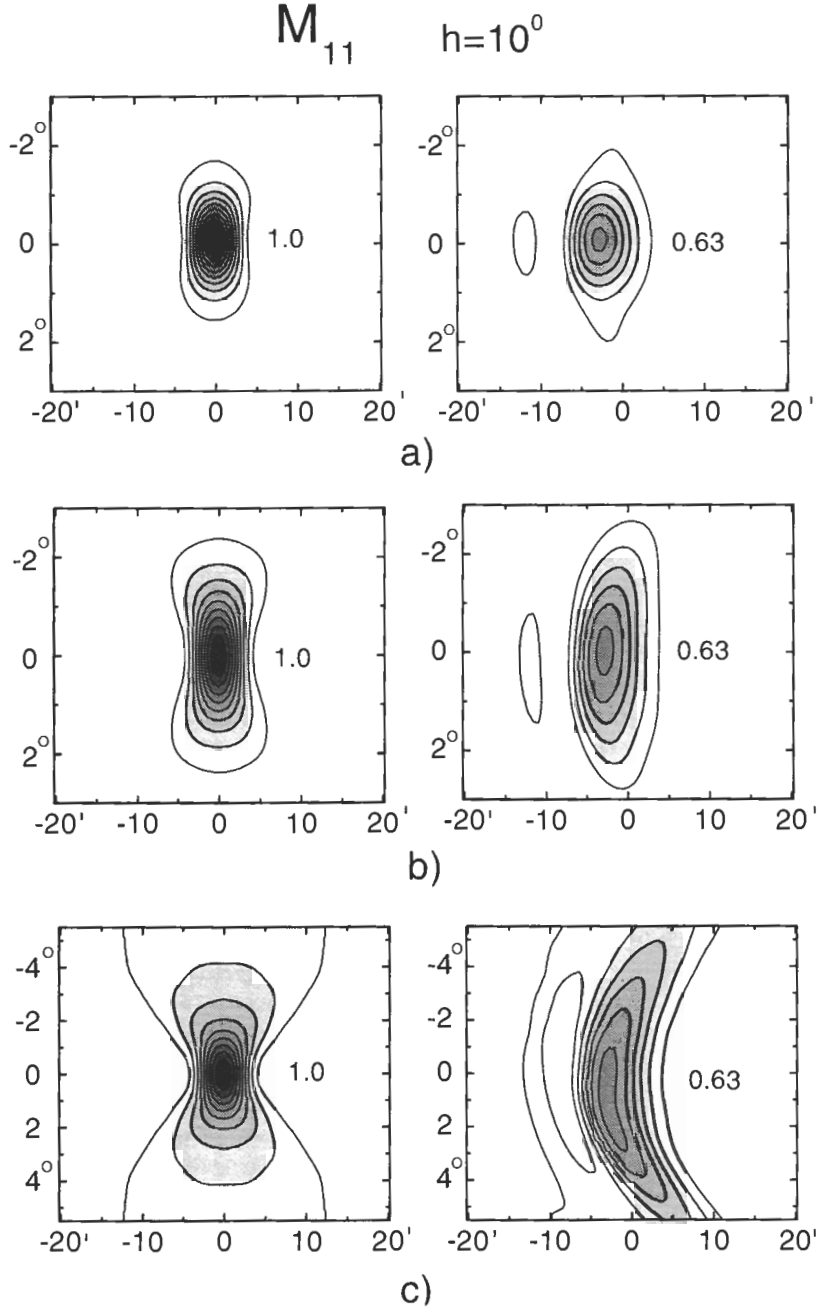

Figure 5: *Power BPs (M_{11}) at the wavelength $\lambda 32$ cm, computed: a) — in the diffraction approximation by formulae (1-8), b) — in the approximation of geometrical optics by formula (8) for phase Φ, c) — in the approximation of geometrical optics by formula (9) for phase Φ. The BPs are normalized to $M_{11}(0,0)$, the numbers designate their maximum values. The isophotes are plotted with a step of 0.1. $\Delta x = 0$ (left), $\Delta x = 5\lambda$ (right).*

elevation, and at $h = 0°$ the vertical BP of the radio telescope is fully determined by the effective vertical size of the panel. At short wavelengths, where the influence of the diffraction effects is insignificant and the approximation of geometrical optics is satisfied, the narrowing of the BP is due to more correct provision for the width of the ring of the primary mirror (panel size). With increasing wavelength, the influence of diffraction effects becomes noticeable, which causes additional narrowing of the BP and also some displacement (λ 32 cm) of the BP maximum in the vertical plane.

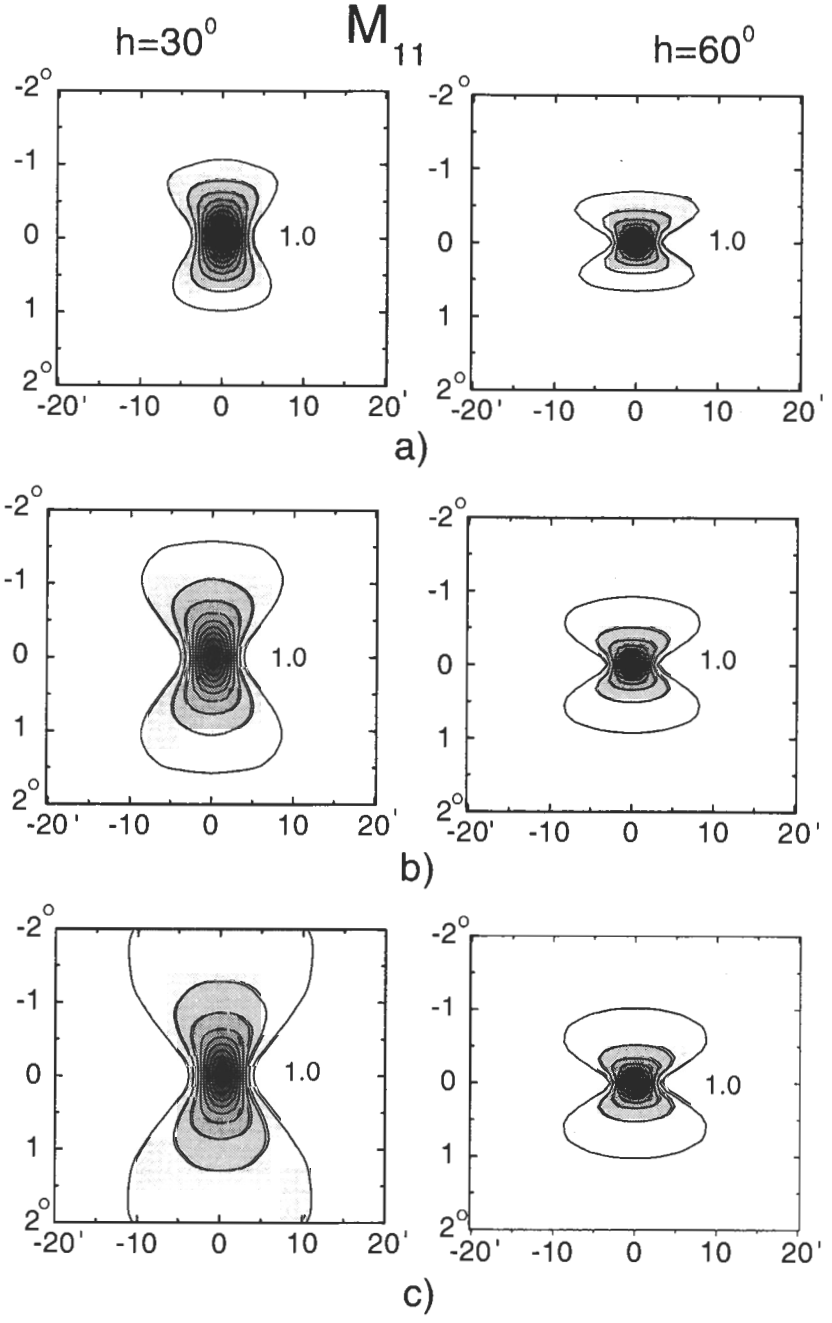

Figure 6: *Power BPs (M_{11}) at the wavelength $\lambda 32$ cm, computed: a) — in the diffraction approximation by formulae (1–8), b) — in the approximation of geometrical optics by formula (8) for phase Φ, c) — in the approximation of geometrical optics by formula (9) for phase Φ. The BPs are normalized to $M_{11}(0,0)$, the numbers designate their maximum values. The isophotes are plotted with a step of 0.1 (Δ x = 0).*

4. Computation of polarization characteristics of RATAN-600 with taking account of diffraction effects

The calculation of the Mueller matrix elements M_{41} and M_{32} was performed by the formulae of Esepkina et al. (1972):

$$M_{41} = [(f^*_{xx} f_{xy} - f_{xx} f^*_{xy}) + (f^*_{yx} f_{yy} - f_{yx} f^*_{yy})]/2, \quad (10)$$

$$M_{32} = [(f^*_{xx} f_{xy} + f_{xx} f^*_{xy}) - (f^*_{yx} f_{yy} + f_{yx} f^*_{yy})]/2. \quad (11)$$

To calculate f_{ij}, formulae (2 — 8) were used. The computations were carried out for the BPs of the primary feeds symmetrical in the E and H planes. The

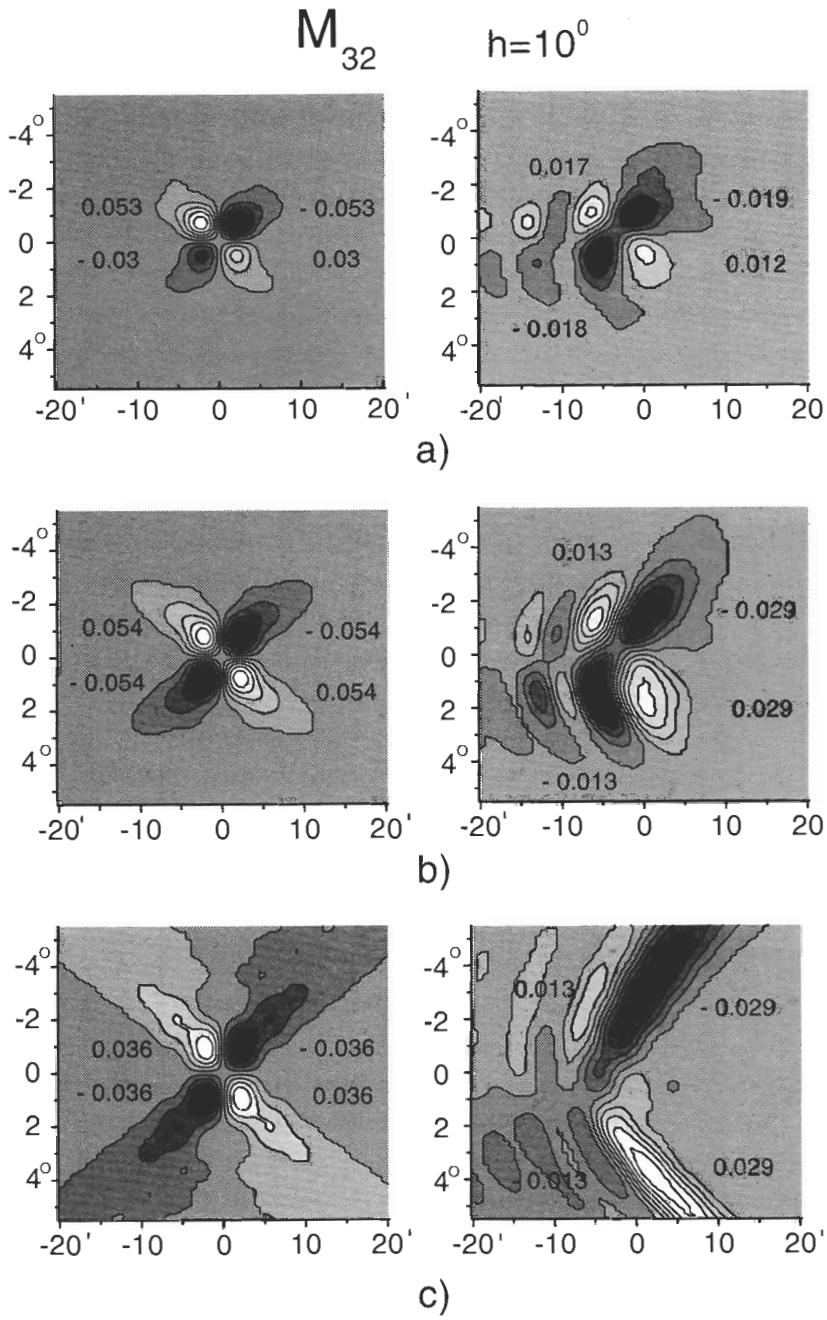

Figure 7: *Isophotes of the element M_{32} at λ 32 cm, computed: a) — in the diffraction approximation by formulae (1–8), b) — in the approximation of geometrical optics by formula (8) for phase Φ, c) — in the approximation of geometrical optics by formula (9) for phase Φ. $\Delta x = 0$ (left), $\Delta x = 5\lambda$ (right). The elements M_{32} are normalized to $M_{11}(0,0)$, the numbers indicate their maximum and minimum values. The light regions correspond to positive M_{32} values, the dark regions — to negative. The isophotes are plotted with a step of 0.01 ($\Delta x = 0$) and a step of 0.005 ($\Delta x = 5\lambda$).*

isophotes of the elements M_{32}, M_{41} at λ32 cm for the elevations $10°, 30°, 60°$ are shown in Figs. 7, 8, 9, 10. The left panels of Figs. 7 and 9 illustrate the case of the focused antenna; the transversal displacement of the primary feed from the focus by 5λ is shown in the right panels. The Mueller matrix elements in Figs. 7(a)—10(a) are computed in the diffraction approximation by formulae ((2)—(8)), in Figs.7b —10b they are given in the approximation of geometrical optics with the application of formula (8) for the

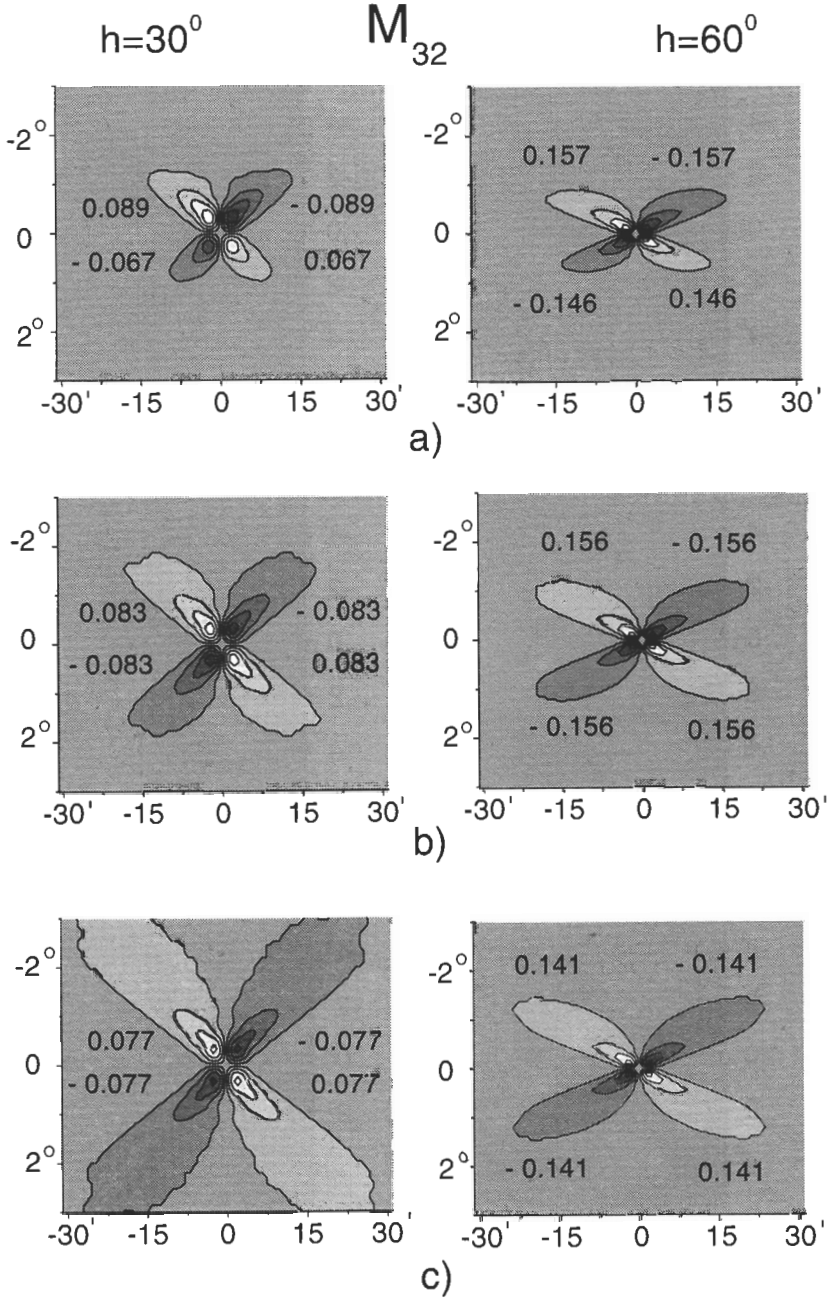

Figure 8: *Isophotes of the element M_{32} at λ 32 cm, computed: a) — in the diffraction approximation by formulae (1–8), b) — in the approximation of geometrical optics by formula (8) for phase Φ, c) — in the approximation of geometrical optics by formula (9) for phase Φ. The elements M_{32} are normalized to $M_{11}(0,0)$, the numbers indicate their maximum and minimum values. The light regions correspond to positive M_{32} values, the dark regions — to negative. The isophotes are plotted with a step of 0.02 ($h = 30°$) and with a step of 0.035 ($h = 60°$) ($\Delta x = 0$).*

phase calculation, Figs.7c —10 shows them in the approximation of geometrical optics using formula (9). The values of the elements M_{41} and M_{32} are normalized to $M_{11}(0,0)$, the figures present their maximum (minimum) values. The light areas correspond to positive values of matrix elements, the dark areas — to negative.

In Fig. 11 are given the maximum values of the matrix elements M_{41}, M_{32} as a function of the source elevation at λ 32 cm, which are computed in the dif-

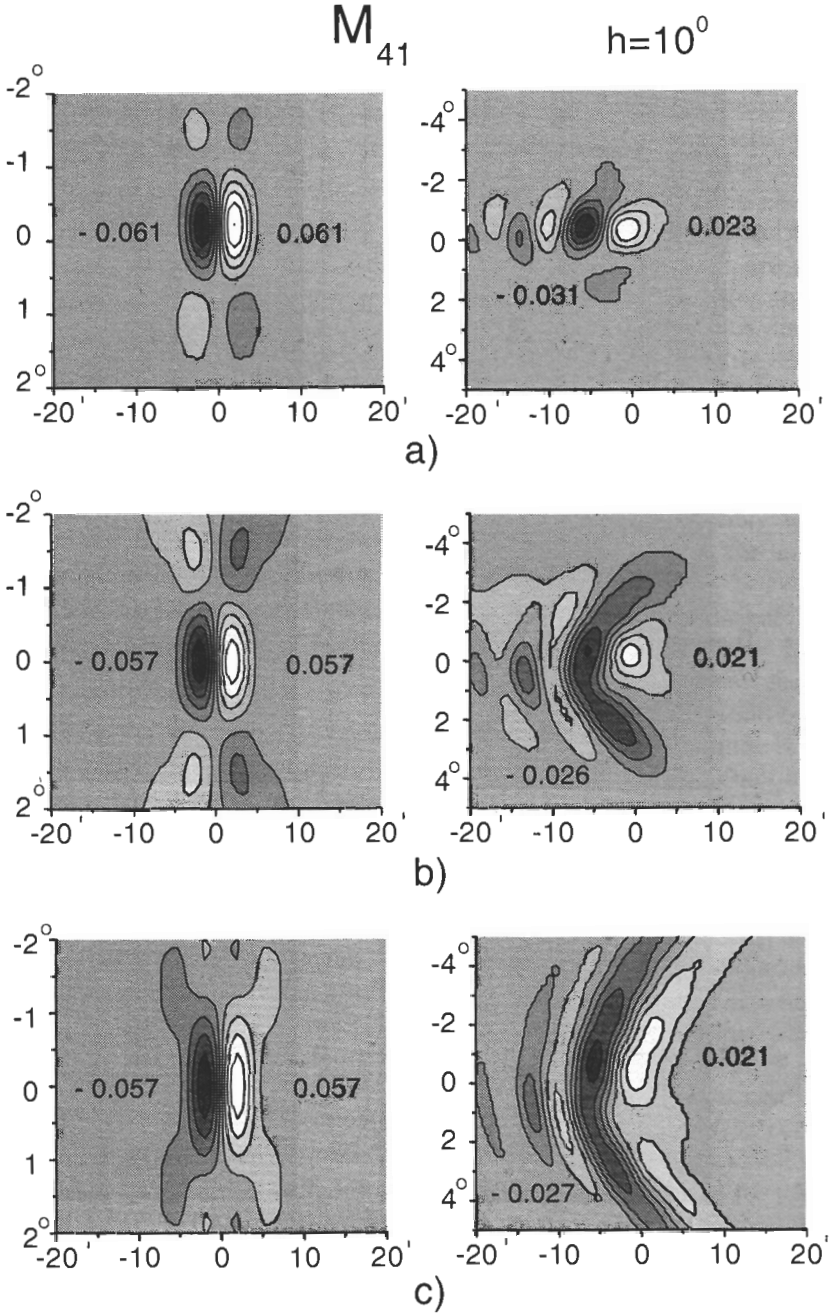

Figure 9: *Isophotes of the element M_{41} at λ 32 cm, computed: a) — in the diffraction approximation by formulae (1-8), b) — in the approximation of geometrical optics by formula (8) for phase Φ, c) — in the approximation of geometrical optics by formula (9) for phase Φ. $\Delta x = 0$ (left), $\Delta x = 5\lambda$ (right). The elements M_{41} are normalized to $M_{11}(0,0)$, the numbers indicate their maximum and minimum values. The light regions correspond to positive M_{41} values, the dark regions — to negative. The isophotes are plotted with a step of 0.013 ($\Delta x = 0$) and a step of 0.007 ($\Delta x = 5\lambda$).*

fraction approximation. The solid line corresponds to ${M_{32}}^{max}$ in the upper half-plane, the dashed line to ${M_{32}}^{max}$ in the lower half-plane.

As one can see from the isophotes displayed in Figs.7—10, the matrix elements M_{32} and M_{41} undergo the same variations as the element M_{11}, namely, with correct allowance made for the vertical size of the panel and diffraction effects in the Fresnel zone they become less extended. The effect is the more significant the lower the elevation of the source. Be-

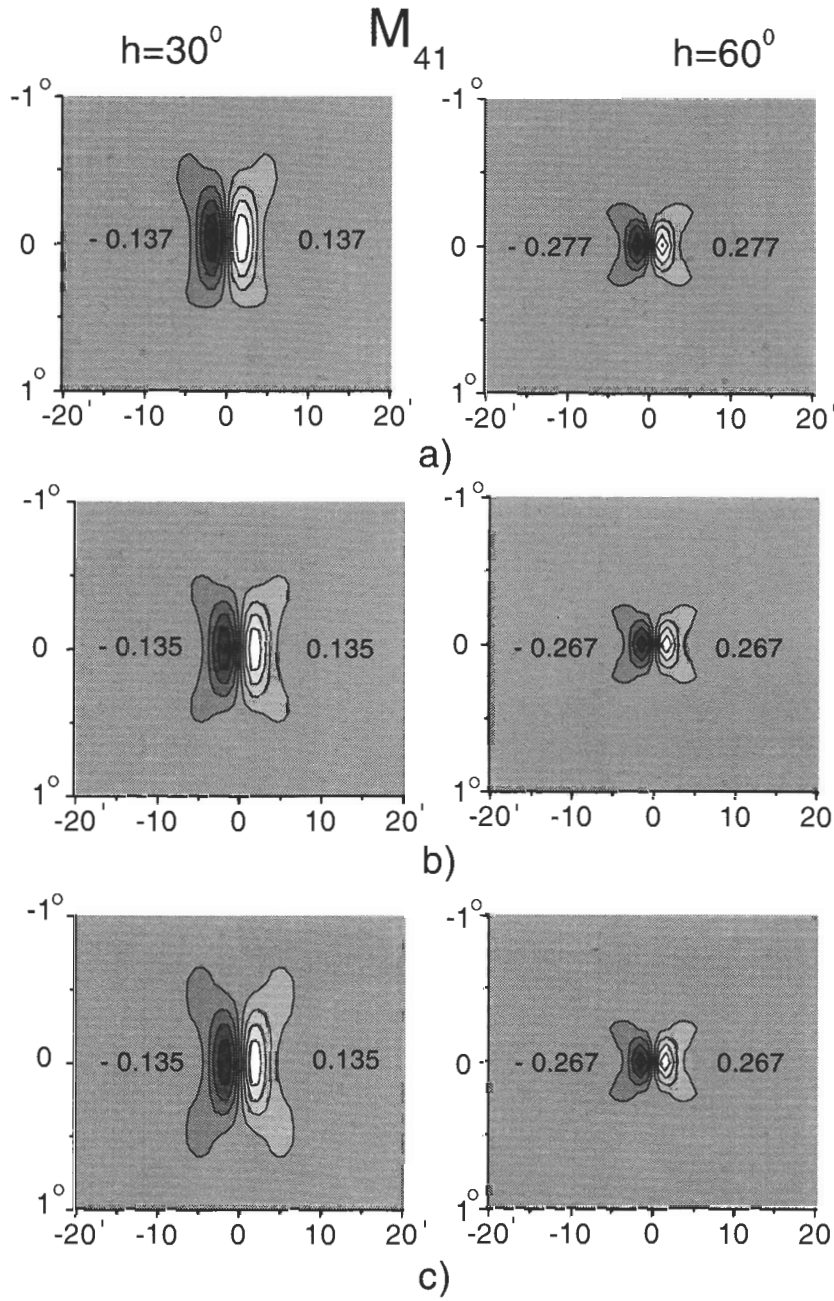

Figure 10: *Isophotes of the element M_{41} at λ 32 cm, computed: a) — in the diffraction approximation by formulae (1-8), b) — in the approximation of geometrical optics by formula (8) for phase Φ, c) — in the approximation of geometrical optics by formula (9) for phase Φ. The elements M_{41} are normalized to $M_{11}(0,0)$, the numbers indicate their maximum and minimum values. The light regions correspond to positive M_{41} values, the dark regions — to negative. The isophotes are plotted with a step of 0.03 ($h = 30°$) and with a step of 0.06 ($h = 60°$) ($\Delta x = 0$).*

sides, in the elements M_{32} and M_{41} other variations are observed, namely, their maximum (minimum) values change as compared to those derived in the approximation of geometrical optics. The maximum (minimum) values of the element M_{41} increases from 3% to 10% depending on the wavelength and the elevation of the source. These changes are the more significant the smaller the angle h. The relation $|{M_{41}}^{min}| = |{M_{41}}^{max}|$ for the focused antenna is not affected by taking into account of the diffraction

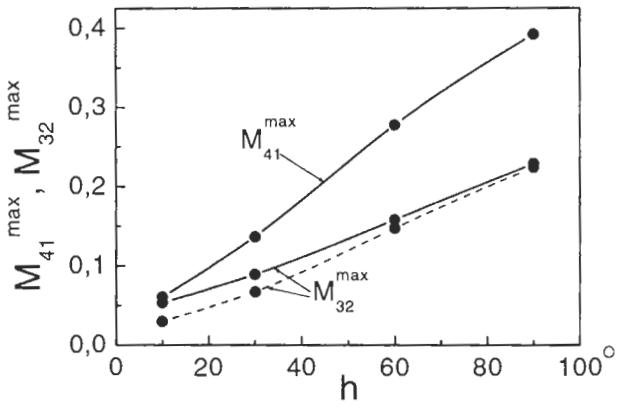

Figure 11: *Maximum values of the matrix elements M_{41} and M_{32} at λ 32 cm computed in the diffraction approximation and as dependent on the elevation h of the source. The solid line refers to $M_{32}{}^{max}$ in the upper half-plane, the dashed line to $M_{32}{}^{max}$ in the lower half-plane.*

effects.

The element M_{32} is a quadrupole with two positive and two negative extrema. In the approximation of geometrical optics, the antenna being focused, the maximum and minimum values of M_{32} are equal in magnitude. Calculations from formula (8) lead to an increase in their magnitudes, basically at low angles, as compared to the values derived via formula (9), the antisymmetry of the element M_{32} is, however, preserved, $(|M_{32}{}^{min}| = |M_{32}{}^{max}|$. With allowance for the diffraction effects, upset of antisymmetry of the element M_{32} about the central horizontal section (X=0) takes place. The maximum (minimum) values of M_{32} in the upper half-plane differ from the minimum (maximum) values of the lower half-plane in magnitude. As calculations have shown, these discrepancies are $1 \div 6\%$ at short wavelengths ($\lambda \leq$ 8 cm) and from 3 % to 50 % at long wavelengths. The strongest disturbance of antisymmetry of the element M_{32} manifests itself at the wavelength λ32 cm at the elevations $h < 30°$ (up to 50%) (Fig. 11). Similar effects are observed both with the focused antenna and in the presence of aberrations in the antenna system.

The disturbance of antisymmetry of the element M_{32} with respect to the central horizontal section is connected with spurious polarization effects of the secondary mirror, which are most pronounced at low elevations and also with increasing influence the vertical size of the panel has on the BP. The disturbance is the stronger the longer the wavelength, because the effective vertical size of reflecting elements of the main mirror and also the non-symmetry of the amplitude-phase field distribution in its vertical aperture caused by the non-symmetry of the secondary mirror increase.

Disturbance of antisymmetry of the element M_{32} is also observed at a considerable displacement of the feed from the focus at elevations close to zenith, where the antenna has a larger aberration-free zone (Stotsky, 1972). So at elevations close to 90° at λ1 cm transversal displacement of the feed from the focus by $100 \div 150\lambda$ ($1 \div 1.5$ m) are possible (Majorova, Khaikin, 2000). Provision for the diffraction effects leads to the fact that at such displacements the values of $|M_{32}{}^{max}|(|M_{32}{}^{min}|)$ in the upper half-plane may exceed those of $|M_{32}{}^{min}|(|M_{32}{}^{max}|)$ in the lower half-plane by 25 % at λ1 cm, whereas this excess for the focused antenna is no larger than 0.06 %. However, the absolute magnitudes of $|M_{32}{}^{max}|(|M_{32}{}^{min}|)$ at $\Delta x = 1 \div 1.5$ m considerably decrease as compared to their values obtained in the approximation of geometrical optics (Fig. 12).

Fig. 12 shows the relation $M_{11}{}^{max} = \mathrm{f}(\Delta x)$, $M_{32}{}^{max} = \mathrm{f}(\Delta x)$, $M_{41}{}^{max} = \mathrm{f}(\Delta x)$ (the so-called aberration curves) at the wavelength λ1 cm for $h = 90°$. The solid lines correspond to the diffraction approximation, the dashed lines to the approximation of geometrical optics. As it can be seen from the figures, allowance for the diffraction effects causes narrowing of the aberration-free zone of the radio telescope near zenith. This is connected with the fact that at very large displacements of the primary feed from the focus the contribution of the antenna edges, where the non-symmetry of the vertical field distribution of the primary mirror is a maximum because of underirradiation of the upper edge of the secondary mirror (Korzhavin, 1979). For the elevations $h < 80°$, where the aberration-free zone of the antenna is not large ($< 10\lambda$), the aberration curves computed with taking account of the diffraction effects in the space between the secondary and the primary mirrors completely coincide with the aberration curves calculated in the approximation of geometrical optics without allowance for the vertical size of the panel (Majorova, Khaikin, 2000).

5. Estimation of the proportion of spurious polarization from the antenna on passage of an extended source across the BP of the radio telescope

Let us estimate the proportion of spurious polarization from the antenna as an extended object passes across the BP of the radio telescope RATAN-600. Dwell upon the case of symmetrical E and H planes of the BP of the primary feeds. Etended sources were modeled by Gaussians whose sizes were somewhat larger than those of the power BP of the radio telescope at a given wavelength. The portion of spurious

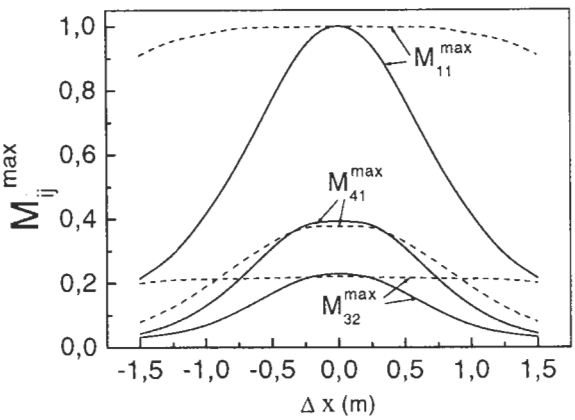

Figure 12: *Relationship between $M_{11}{}^{max}$, $M_{41}{}^{max}$ and $M_{32}{}^{max}$ and transversal displacement Δx of the primary feed from the focus in the diffraction approximation (solid line) and approximation of geometrical optics (dashed line).*

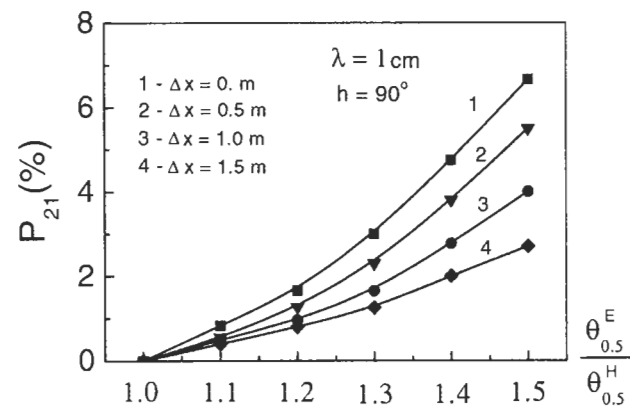

Figure 13: *Portion of linear spurious polarization P_{21} at $\lambda 1$ cm when crossing the BP by an extended source specified by a Gaussian $3' \times 3'$ (in half-width) depending on the ratio of BP half-widths in the E and H planes at different transversal displacements of the horn from the focus.*

polarization P_{ij} was computed as the ratio of the maximum value of convolution of the element M_{ij} with a Gaussian to the maximum value of convolution of the element M_{11} with the same Gaussian.

The computation was carried out in the whole range of wavelengths of RATAN-600 (λ = 1, 4, 8, 16, 32 cm) at the elevations $10°, 30°, 60°, 90°$ for the focused antenna and with longitudinal displacements of the primary feed from the focus. At short wavelengths the value of displacement of the primary feed from the focus was constrained by the drop of signal to a level of 0.4 from the maximum BP of the focused antenna, at long wavelengths — by the dimensions of the carriage (1 m–1.6 m depending on the type of the feed).

The calculations have shown that the portion of spurious polarization P_{41} only slightly depends on wavelength, but significantly depends on elevation of an observed source. At $h = 10°$, it does not exceed 0.7%, at $h = 30°$ — 2%, at $h = 60°$ — 3%. P_{41} reaches the highest values at elevations close to 90°. These values are $3 \div 5$ % at $\lambda = 1 \div 4$ cm at displacements $\Delta x = 20 \div 100\lambda$.

Convolution of the Gaussian with the matrix element M_{32} computed in the approximation of geometrical optics yields a zero value. Provision for the diffraction effects leads to disturbance of antisymmetry and, as a consequence, to the appearance of spurious polarization both for the focused antenna and for the antenna with aberrations. The portion of spurious polarization P_{32} does not exceed $0.1 \div 0.2$ % at $\lambda = 1 \div 1.38$ cm even at a large displacement of the primary feed from the focus (up to 1.5 m). At the wavelengths $\lambda = 4 \div 32$ cm P_{32} does not exceed 1.6 % with the focused antenna and 4 % in the presence of transversal aberrations. The proportion of spurious polarization grows with increasing elevation of the source and reaches a maximum ($1 \div 4$ %) at $h = 60° \div 90°$.

Let us compute the matrix elements M_{21} and M_{31} and estimate the share of spurious polarization P_{21} and P_{31}, caused by the non-symmetry of the BP of the horns in the E and H planes as an unpolarized extended source passes across the BP of the radio telescope.

The computation of M_{21} and M_{31} was performed via the formulae (Esepkina, 1972)

$$M_{21} = [(f^*_{xx} f_{xx} + f_{yx} f^*_{yx}) - (f^*_{xy} f_{xy} + f_{yy} f^*_{yy})]/2, \quad (12)$$

$$M_{31} = [(f^*_{xx} f_{xy} + f_{xx} f^*_{xy}) + (f^*_{yx} f_{yy} + f_{yx} f^*_{yy})]/2. \quad (13)$$

To calculate f_{ij}, formulae (2 — 8) were used.

The values of these elements are equal to zero when the BPs of the horns are symmetrical about the polarization. The proportion of linear polarization associated with the asymmetry of the BPs of the horns in the E and H planes P_{21} and P_{31} was estimated by means of convolution of the elements M_{31} and M_{21} with Gaussians whose half-width are $3' \times 3'$. The computations were performed for the wavelength $\lambda 1$ cm at $h = 90°$. The ratio of the half-widths of the horn BPs in the E and H planes changed from 1.0 to 1.5. The share of spurious linear polarization P_{31} here was not greater than 0.05 %. The relations between P_{21} and the ratio of the half-widths of the horn BPs in the E and H planes at different displacement of the horn from the focus are exhibited in Fig. 13.

Thus the calculations carried out make it possible

to declare that the portion of spurious linear polarization from the antenna will not exceed 1% if the non-symmetry of the horn BP in the E and H planes does not exceed 10%.

6. Conclusions

The calculations carried out with provision for the diffraction effects in the space between the secondary and primary mirrors and also more correct allowance for the vertical size of the panel made possible revision of the shape of the BP of the radio telescope RATAN-600 both in intensity and polarization. The power beam patterns of the radio telescope (M_{11}) and the Mueller matrix elements M_{32}, M_{41} computed with allowance made for these effects have a smaller extent in the verical plane than those obtained by Esepkina et al. (1979b; 1980). The reduction of the solid angle taken by the BP at a level of 0.3 and below proved to be the more considerable the lower elevation of the source and the longer wavelength. From this it follows that at long wavelengths for elevations below 30° the effect of confusion will be far weaker than it was assumed earlier. Variations of the size and shape of the BP is observed both for the focused antenna and in the presence of aberrations. Provision for the diffraction effects at long wavelengths causes not only narrowing of the BP but also displacement of its maximum in the vertical plane. This effect manifests itself at sufficiently low angles in connection with non-symmetry of the secondary mirror. At elevations close to the zenith, the BPs computed in a diffraction approximation and in an approximation of geometrical optics coincide.

Reference measurements of the verical BPs of RATAN-600 were made with the aid of reference point sources. They showed a very good fit of the computed BPs to the experimental BP up to a level of 0.03 from the maximum BP both for the focused antenna and with displacement of the primary feed from the focus.

Allowance for the diffraction effects leads to some increase in the maximum (minimum) values of the matrix elements M_{32}, M_{41}. Besides, in the element M_{32} disturbance of antisymmetry with respect to the central horizontal section occurs. This causes spurious polarization in observations of extended sources, which does not exceed 2% for the focused antenna at long wavelengths and 0.1% at 1 cm. The disturbance of antisymmetry of the element M_{32} is also observed at sufficiently large displacements of the primary feed from the focus near the zenith. The spurious polarization value in observations of extended objects only slightly depends on wavelength and is not higher than 3% for the focused antenna and 5% at large displacements of the feed from the focus (up to 100λ at the wavelength 1 cm). Provision for the diffraction effects results in narrowing of the aberration-free zone of the antenna near the zenith. Calculations of the Mueller matrix elements at ultimate displacements of the feed from the focus yield data which are of importance in designing focal arrays and opting for their dimensions.

The proportion of spurious polarization related to non-symmetry of the horn BPs in the E and H planes as an extended unpolarized source passes across the BP is estimated. The calculations have shown that the portion of spurious linear polarization from the antenna in the investigation of the relic background fluctuations with RATAN-600 (experiment "Cosmological gene") will not exceed 1% even at great displacements of the primary feeds from the focus if the asymmetry of the horn BPs in the E and H planes is not higher than 10%.

The programme of computation of the two-dimensional BP of RATAN-600 created on the already existing programmes can be useful in modeling deep surveys. The good fit of the computation results to the experimental data will enable, with the aid of this programme, deeper processing of data and "cleaning" records from strong background sources passing across the BP far off its axis.

Acknowledgements. The author is thankful to A.N. Korzhavin, Yu.N. Parijskij and S.A. Trushkin for discussion of results and helpful comments.

References

Abramov V.I., Vinyajkin E.N., 1985, Astrofiz. Issled. (Izv.SAO), **19**, 93

Bakhvalov N.S., Vasil'eva L.G., Esepkina N.A., Soboleva N.S., Temirova A.V., 1973, Astrofiz. Issled. (Izv.SAO), **5**, 135

Bogod V.M., Gelfreikh G.B., Korzhavin A.N., Pustil'nik L.A., 1988, Preprint SAO, No. 22

Braude B.V., Esepkina N.A., Kajdanovskij N.L., Parijskij Yu.N., Shivris O.N., 1972, Izv. MAO, **188**, 40

Esepkina N.A., Kajdanovskij N.L., Kuznetsov B.V., Kuznetsova G.V., Khajkin S.Eh., 1961, Radiotekhnika i elektronika, **6**, No.12, 1947

Esepkina N.A., Vasil'ev B.A., Vodovatov I.A., Vysotskij M.G., Vinogradov G.K., 1977, Radiotekhnika i elektronika, **22**, No 7, 1984

Esepkina N.A., 1972, Astrofiz. Issled. (Izv.SAO), **4**, 157

Esepkina N.A., Vasil'ev B.A., Vodovatov I.A., Vysotskij M.G., 1979a, Astrofiz. Issled. (Izv.SAO). **11**, 197

Esepkina N.A., Bakhvalov N.S., Vasil'ev B.A., Vasil'eva L.G., Temirova A.V., 1979b, Astrofiz. Issled. (Izv.SAO), **11**, 182

Esepkina N.A., Bakhvalov N.S., Vasil'ev B.A., Vasil'eva L.G., Vodovatov I.A., Temirova A.V., 1980, Astrofiz. Issled. (Izv.SAO), **12**, 106

Esepkina N.A., Bakhvalov N.S., Vasil'ev B.A., Vasil'eva L.G., Temirova A.V., 1982, Astrofiz. Issled. (Izv.SAO), **15**, 151

Gelfreikh G.B., 1977, Astrofiz. Issled. (Izv.SAO), **9**, 89

Gelfreikh G.B., 1972, Izv.MAO, **188**, 139
Gelfreikh G.B., Opeikina L.V., 2000, Bull. Spec. Astrophys. Obs., **50**, 104
Golubchina O.A., Golubchin G.S., 1981, Astrofiz. Issled. (Izv.SAO), **14**, 125
Korzhavin A.N., 1977, Astrofiz. Issled. (Izv.SAO), **9**, 71
Korzhavin A.N., 1979, Astrofiz. Issled. (Izv.SAO), **11**, 170
Majorova E.K., Stotsky A.A., 1981, Astrofiz. Issled. (Izv.SAO), **13**, 117
Majorova E.K., Stotsky A.A., 1982, Astrofiz. Issled. (Izv.SAO), **15**, 117
Majorova E.K., Khaikin V.B., 2000, Bull. Spec. Astrophys. Obs., **50**, 91
Parijskij Yu.N., 2000, Astron. and Astrophys. Transactions, **19**, 265
Stotsky A.A., 1972, Izv.MAO, **188**, 63
Temirova A.V., 1983, Astrofiz. Issled. (Izv.SAO), **17**, 131
Temirova A.V., 1985, Astrofiz. Issled. (Izv.SAO), **19**, 101
Verkhodanov O.V., Erukhimov B.L., Monosov M.L., Chernenkov V.N., Shergin V.S., 1993, Bull. Spec. Astrophys. Obs., **36**, 132